Journal of Power Sources 196 (2011) 4483–4490

Contents lists available at ScienceDirect

Journal of Power Sources

journal homepage: www.elsevier.com/locate/jpowsour

Plasma-grafted alkaline anion-exchange membranes based on polyvinyl chloride for potential application in direct alcohol fuel cell

Jue Hu [a,*], Chengxu Zhang [a,*], Jie Cong [a], Hirotaka Toyoda [b], Masaaki Nagatsu [c], Yuedong Meng [a]

[a] Institute of Plasma Physics, Chinese Academy of Sciences, P.O. Box 1126, Hefei, PR China
[b] Department of Electrical Engineering and Computer Science, Nagoya University, Japan
[c] Nanovision Science Section, Graduate School of Science and Technology, Shizuoka University, Japan

ARTICLE INFO

Article history:
Received 11 December 2010
Received in revised form 7 January 2011
Accepted 7 January 2011
Available online 19 January 2011

Keywords:
Alkaline anion-exchange membrane
Direct alcohol fuel cell
Plasma-grafting
Polyvinyl chloride powder
Vinylbenzyl chloride

ABSTRACT

Plasma grafting is employed to prepare alkaline anion-exchange membranes in this study. The attenuated total reflection Fourier transform infrared spectroscopy, X-ray photoelectron spectroscopy and thermo gravimetric analysis demonstrate that the benzyltrimethylammonium cationic groups are successfully introduced into the polyvinyl chloride matrix via plasma grafting, quaternization and alkalization. The plasma-grafted alkaline anion-exchange membrane exhibits a satisfactory ionic exchange capacity (1.01 mmol g^{-1}), thermal stability, mechanical property, ionic conductivity (0.0145 S cm^{-1}) and methanol permeability (9.59×10^{-12} m^2 s^{-1}), suggesting a great potential for application in direct alcohol fuel cells. The open circuit voltage of air-breathing ADAFC using plasma-grafted alkaline anion-exchange membrane is 0.796 V with 1 M EtOH solution at ambient temperature.

1. Introduction

Direct alcohol fuel cells (DAFCs) are expected to be promising power sources ranging from automotive to portable electronic device applications due to their high power density and low environmental pollution [1–4]. Proton exchange membrane direct alcohol fuel cells (PEMDAFCs) have been extensively explored thanks to the numerous advantages. However, there are still scientific and technological difficulties that impede their widespread commercialization: high cost for using noble metals as catalyst, fuel permeation and slow oxidation kinetics of alcohol [1,5]. To overcome these problems, it is natural to consider an alkaline analogue of DAFC. Several merits for alkaline direct alcohol fuel cells (ADAFCs) have been suggested: (1) potential to forego noble metal catalysts [6,7]; (2) lower fuel permeability [3]; (3) lower overpotentials associated with many electrochemical reactions at high pH [8,9]; (4) less serious corrosion in alkaline environment [8]; and (5) a significant change in water management [8]. There has been a growing interest in the development of alkaline anion-exchange membranes (AAEMs), which served dual functions of hydroxide ion conducting and fuels separating, and, as a result, seriously affected the performance of ADAFCs.

Significant effort has been focused on the preparation of AAEMs by performing a chloromethylation reaction on the polymer to form benzylic chloromethyl groups and then converting the benzylic chloromethyl groups into benzyltrimethylammonium cationic groups in subsequent quaternization and alkalization steps [5,10–13]. However, the chloromethyl ether, which was usually used in the chloromethylation reaction as a carcinogen, is potential harmful to human health [14]. Grafting of vinylbenzyl chloride (VBC) onto polymer matrix has been proved to be an effective way to avoid using chloromethyl ether [15–18]. Nevertheless, due to the high irradiation damage of the polymer matrix, AAEMs produced by radiation-grafting are promising only when fully fluorinated base films are used [15]. Plasma grafting is a mild and efficient method for introducing functional groups onto the surface of the polymer matrix, and, as a result, nonfluorinated base polymers can be used [19]. In plasma grafting process, exciting species such as electrons, ions and neutral particles within plasma bombard with the polymer surface and create active sites for binding of functional groups. Since the chemical and physical modifications occur only on the polymer surface, the use of polymer powders instead of polymer films as the polymer matrix seems to be a better choice. Polyvinyl chloride (PVC) powder, as an important commercial polymer, has been employed in this study due to its good solubility in certain solvents and film forming characteristics.

The purpose of the present study is to prepare and characterize the novel plasma-grafted AAEMs for potential application in ADAFCs. The physicochemical and electrochemical characteristics,

* Corresponding authors. Tel.: +86 551 5591378; fax: +86 551 5591310.
E-mail addresses: hujue@ipp.ac.cn (J. Hu), chxzhang@ipp.ac.cn (C. Zhang).

0378-7753/$ – see front matter © 2011 Elsevier B.V. All rights reserved.
doi:10.1016/j.jpowsour.2011.01.034

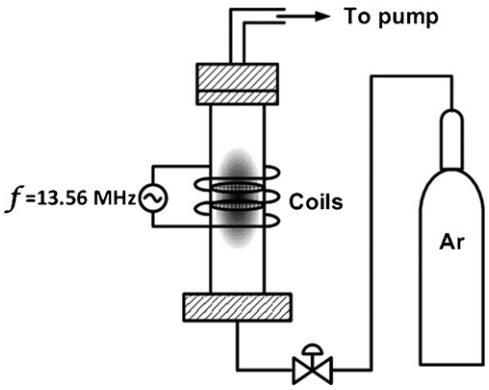

Fig. 1. Schematic diagram of the apparatus used for plasma grafting.

namely water uptake, ionic exchange capacity, thermal stability, chemical stability, mechanical property, ionic conductivity and methanol permeability, were evaluated.

2. Experimental part

2.1. Preparation of plasma-grafted membrane

Plasma device for PVC powder (particle size around 50 μm, Shenma, China) treatment consists of a cylindrical Pyrex glass vacuum tube with a diameter of 55 mm and a height of 250 mm, shown in Fig. 1. PVC powders were placed between two pieces of Nylon screens in the middle of the Pyrex glass tube. The inductively coupled plasma (ICP) sustained by a 13.56 MHz power supply inside the brass coil, using argon as the working gas. The flow rate of argon was controlled by gas mass flow controller. The plasma treatment conditions were fixed: argon plasma under the discharge power of 150 W, total pressure of 30 Pa and treatment time of 10 min.

After the argon plasma treatment, the plasma treated PVC powders were rapidly removed into a conical flask and then excess VBC (95%, Alfa Aesar®) was injected into the grafting reactor. The mixture was stirred for 24 h at 60 °C. The obtained plasma-grafted polymer (PVC-*g*-PVBC, P1) was washed with deionized water for several times to remove any trapped VBC molecule, and then dried in vacuum oven for 48 h at 60 °C. Dried P1 powders (1 g) were dissolved in tetrahydrofuran (THF, Shanghai Chemical Reagent Store, China) to form a 10 wt% solution. The solution of P1 in THF was cast onto a flat, clean glass plate and placed in a vacuum oven at 60 °C for 24 h, after which the film was removed from the glass plate by immersing them in deionized water.

2.2. Quaternization and alkalization of plasma-grafted membranes

The plasma-grafted P1 membranes were soaked in 33 wt% trimethylamine (TMA, Shanghai Chemical Reagent Store, China) aqueous solution at room temperature for 48 h. After soaking, the quaternized membranes (PVC-*g*-QPVBCTMACl, P1NCl) were washed with deionized water to remove excess TMA solution. The P1NCl membranes were immersed in 1 M KOH solution at room temperature for 48 h to convert the membranes from the Cl^- form into the OH^- form. Then, the alkalized membranes (PVC-*g*-QPVBCTMAOH, P1NOH) were washed by deionized water to remove any trapped KOH and finally immersed in deionized water for at least 48 h with frequent water changes.

The reaction sequence of the synthesis of the P1NOH membrane is shown in Fig. 2.

2.3. Chemical structure characterization measurements

The chemical structure and composition of the obtained membranes were analyzed by attenuated total reflection Fourier transform infrared spectroscopy (ATR-FTIR) and X-ray photoelectron spectroscopy (XPS). All the samples were dried in a vacuum oven at 60 °C for 12 h. The ATR-FTIR analysis was performed in the range of 4000–670 cm^{-1} on Nicolet NEXUS 870 spectrometer. The spectra were obtained after 256 scans at 2 cm^{-1} resolution with subtracting the contributions from CO_2 and H_2O (gas). The XPS analysis was carried out using a Thermo ESCALAB 250 spectroscopy at a power of 150 W with a monochromatic Al Kα radiation at 1486.6 eV. The spectrometer energy scale calibration was checked by setting Ag $3d_{5/2}$ = 368.26 eV and the spectra were calibrated with respect to the C 1s peak at 284.6 eV. The energy resolution was about 0.6 eV. XPS of P1 and P1NOH membranes were recorded at pass energies of 70 eV for survey spectra and 20 eV for core level spectra. The photoelectrons were detected with a hemispherical analyzer positioned at an angle of 90° with respect to the sample plane. An additional electron gun was used to allow for surface neutralization during the measurements since the membranes were nonconductive. The curves were fitted with symmetrical Lorentz–Gauss functions. The thermo gravimetric analysis (TGA) was used to observe the thermal stability of the obtained dried membranes using DTG-60H (SHIMADZU, Japan) thermal analyzer in flowing nitrogen from ambient temperature to 800 °C at a scanning rate of 10 °C min^{-1}.

2.4. Ion-exchange capacity (IEC) measurements

The ion-exchange capacities (IECs) of the P1NCl and P1NOH membranes were measured by classical back titration method to evaluate the capability of hydroxide ion transport. For IEC measurement, as reported previously [20], three pieces of the dried membrane samples prepared in the same time were accurately weighed and then respectively equilibrated with 25 ml 0.05 M HCl solution for 48 h, after which the HCl solution was back titrated by 0.05 M NaOH solution. IEC values of the samples were calculated as the following relation:

$$\mathrm{IEC\,(mmol\ g^{-1})} = \frac{n_{1,\mathrm{HCl}} - n_{2,\mathrm{HCl}}}{m_{\mathrm{dry}}} \quad (1)$$

where $n_{1,HCl}$ and $n_{2,HCl}$ are the amount (mmol) of hydrochloric acid required before and after equilibrium, respectively, and m_{dry} is the mass (g) of the dried sample. The average value of the three samples calculated from Eq. (1) is the IEC value of the measured membrane.

2.5. Water uptake measurements

The uptake of water in the membrane was carried out by measuring the change of weight between the membrane before and after immersion in deionized water. First, the membrane was soaked in deionized water at room temperature and equilibrated for more than 48 h. The weight of the wet membrane was recorded as a benchmark by measuring after removing excess surface water. The wet membrane was then dried under vacuum at 60 °C until a constant weight was obtained. The weight of the dry membrane was measured, and the water uptake could be calculated using Eq. (2)

$$\text{Water uptake}\ \% = \frac{m_{\mathrm{wet}} - m_{\mathrm{dry}}}{m_{\mathrm{dry}}} \times 100\% \quad (2)$$

where m_{wet} is the mass (g) of a wet membrane and m_{dry} is the mass of a dry membrane.

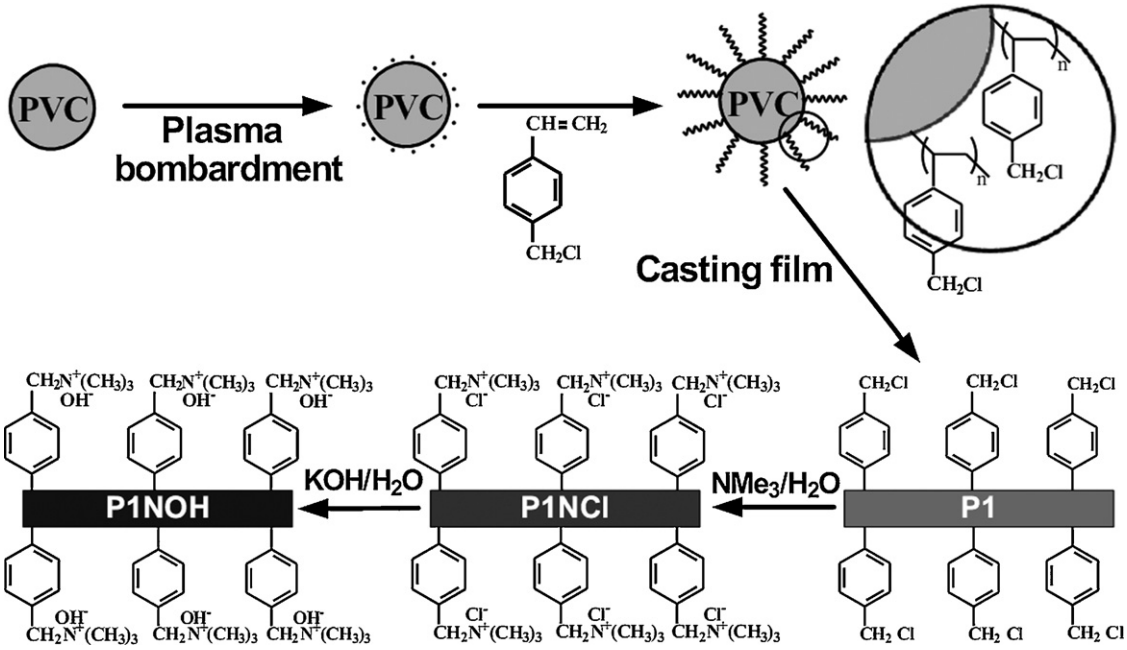

Fig. 2. Synthesis of the plasma-grafted alkaline anion-exchange membranes.

2.6. Ionic conductivity measurements

The hydroxide ion conductivity of the obtained membranes was measured by three-electrode AC impedance spectroscopy,, described in the literature [21,22], using an Autolab potentiostat/galvanostat (IM6e, Zahner, Germany) over a frequency ranging from 0.1 Hz to 1 MHz with oscillating voltage of 10 mV. Before testing, the OH– form of quaternized membrane P1NOH samples (2.0 cm × 4.0 cm) were hydrated in deionized water for at least 48 h until neutral pH was obtained. After by removing the surface water, the hydrated membrane was then rapidly placed between two polytetrafluoroethylene (PTFE) plates, with one side contacted with three parallel platinum wires. The reference electrode (RE) was connected to the inner platinum wire, and the counter electrode (CE) and working electrode (WE) were connected to the outer two platinum wires, respectively. The testing cell was placed in a chamber with deionized water to keep the water content of the membrane constant during the measurements. This method avoids contact resistance effectively and the results are well reproducible in the measurement [21]. The hydroxide ion conductivity σ_{OH^-} could be calculated using the relation:

$$\sigma_{OH^-}\ (S\,cm^{-1}) = \frac{l}{R_m A} \quad (3)$$

where l was the distance (cm) between the working electrode and reference electrode, A was the cross-sectional area (cm^2) of the membrane, and R_m was the membrane resistance (Ω) obtained from the AC impedance data.

2.7. Methanol permeability measurements

The alcohol permeability, such as methanol permeability, was measured by an open circuit potential method as reported in Ref. [21–24], using an Autolab potentiostat/galvanostat (IM6e, Zahner, Germany) at the temperature of 20 °C. Before testing, the OH^- form of quaternized membrane P1NOH samples (3.0 cm × 3.0 cm) were hydrated in deionized water for at least 48 h until neutral pH was obtained. The membrane sample was then clamped between two compartments of a diffusion cell by means of an O-ring seal with the membrane cross-sectional area of 2.0 cm^2 exposed to the solution. Teflon coated magnetic paddles were used in each compartment to ensure uniform mixing during the experiments. The compartment A was loaded with 1 M KOH and 1 M MeOH solution. An equal volume of 1 M KOH solution was present in the compartment B. In the compartment B, a Pt foil was used as CE, a Hg/Hg_2Cl_2, KCl (saturated) electrode was used as RE, and a Pt/C gas diffusion electrode (GDE) with flowing pure O_2, prepared by pasting Pt/C (40 wt%, Johnson Matthey) catalyst on carbon paper (Pt loading of 0.5 mg cm^{-2}), was used as WE. The methanol concentration of compartment B can be estimated by the GDE potential drop from the calibration curve of potential shift against methanol concentration. The method to establish the calibration curve of potential shift against methanol concentration was described in our previous report, with substituting 1 M KOH solution for 0.5 M H_2SO_4 solution [21].

2.8. Oxidation experiments

The chemical stability of membrane was investigated by immersing the samples into 3 wt% H_2O_2 solution at 60 °C for more than 240 h. The 3 wt% H_2O_2 solution was renewed for every 12 h. The weight loss of the sample was measured at certain time intervals.

2.9. Mechanical property measurements

The mechanical properties of obtained membranes before and after water-uptake were analyzed by a Dynamic Mechanical Thermal Analyzer (Q800, TA Instruments, USA) at 23 °C. Test specimens of dried P1 membrane, P1NOH membrane, and water saturated P1 membrane, P1NOH membrane were all 5 mm in width and 14 μm, 15 μm, 14 μm and 20 μm in thickness, respectively. The cross-head speed was 0.5 N min^{-1} with the initial grip distance of 10 mm. Tensile strength (TS), elongation at break (E_b) and tensile modulus were recorded. The date was the average of three trials.

2.10. Cell performance tests

Cell performance tests were carried out with an in-house fabricated air-breathing ADAFC single cell, a theostat (ZX92E,

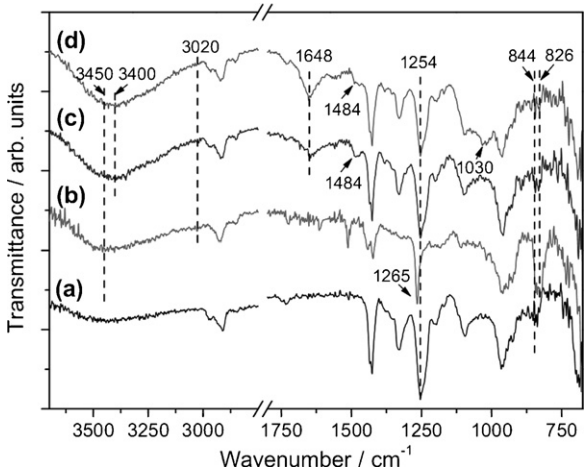

Fig. 3. ATR-FTIR spectra of (a) PVC, (b) P1, (c) P1NCl and (d) P1NOH membranes.

China) and a digital multimeter (17B FLUKE, USA) at ambient temperature. The alkaline DAFC was composed of a membrane electrode assembly (MEA) sandwiched between two stainless steel bipolar plates. Pt black powder (40 wt% Pt, Johnson Matthey) was mixed with isopropanol and sprayed on PTFE treated carbon paper (HCP020P, Hesen) to make an electrode. To prepare the MEA, the P1NOH membrane was sandwiched by the thus-obtained electrodes. The Pt loading in the anode and cathode was 0.40 mg cm^{-2} and 0.20 mg cm^{-2}, respectively. Fuel cell tests were conducted with 1–2 M ethanol (EtOH) solution at a rate of 1.0 ml min^{-1}. Air was supplied to the cathode as the oxidant by natural convection. The ADAFC performance curves were recorded by fixing the load current, which was controlled with a theostat. All the data were collected after the cell performance became stable.

3. Results and discussion

3.1. Chemical structure characterization

The chemical structures of PVC, P1, P1NCl and P1NOH membranes were analyzed by ATR-FTIR spectra, shown in Fig. 3. The absorption at 844 cm^{-1} and 1254 cm^{-1} in the ATR spectrum of PVC related to the C–Cl stretching vibrations and C–H rocking, respectively [25]. The ATR spectrum of P1 showed four bands at 826 cm^{-1}, 1265 cm^{-1}, 3020 cm^{-1} and 3450 cm^{-1}, not present for PVC, assigned to C–H deformation for para-substituted aromatics, CH_2–Cl wag of benzyl chloride groups, aromatic C–H stretches and O–H stretching in H_2O, respectively, suggesting the successful grafting of VBC [20,26,27]. The bands at 1484 cm^{-1}, 1648 cm^{-1} and 3400 cm^{-1} of P1NCl and P1NOH were assigned to C–H bending of trimethylammonium, amide|band and N–H stretching, respectively, indicating the successful quaternization of benzyl chloride groups [21,27–29]. In the spectra of P1NCl and P1NOH, the CH_2–Cl wag of benzyl chloride groups at 1265 cm^{-1} disappeared, confirming the thorough quaternization of P1 membrane. The band at 1030 cm^{-1} in the spectrum of P1NOH membrane, corresponding to the hydroxyl group, verified the introduction of hydroxide ion in the alkalinized membrane [30].

To acquire more information on the chemical structure characteristics of obtained membranes, XPS data of P1 and P1NOH membranes were conducted. As shown in Fig. 4(a) and (b), the C 1s peak could be curve-fitted with three peaks [31–34]: peak (1) at 284.6 ± 0.2 eV attributed to the sp^3 carbon atoms (C–C and C–H) and sp^2 carbon atoms (C=C); peak (2) at 286.1 ± 0.2 eV corresponded to sp^3 carbon bonded to one oxygen atom (C–O), nitrogen atom

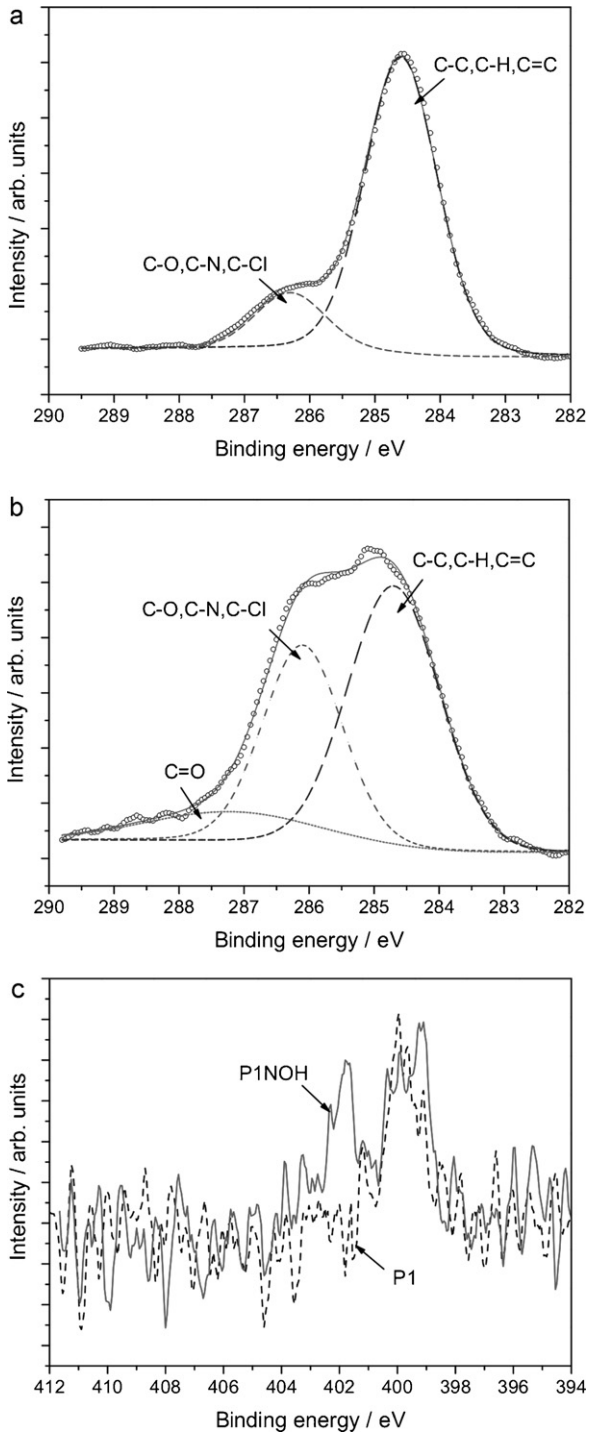

Fig. 4. XPS spectra of C 1s for (a) P1 and (b) P1NOH membranes and N 1s (c) for the P1 and P1NOH membranes.

(C–N) and chlorine atom (C–Cl); peak (3) at 287.2 eV assigned to the oxygenated groups (carbonyl). The huge increase in the C–N, C–O and C–Cl fraction of P1NOH membrane indicates the successful quaternization and alkalization of P1 membrane. Fig. 4(c) shows the N 1s core-level XPS spectra of the P1 and P1NOH membranes. The peak at 401.7 eV for P1NOH membrane was attributed to the positively charged nitrogen (N^+) [35–37]. This may confirm that the quaternary ammonium functional groups have been introduced into the PVC matrix via plasma grafting, quaternization and alkalization.

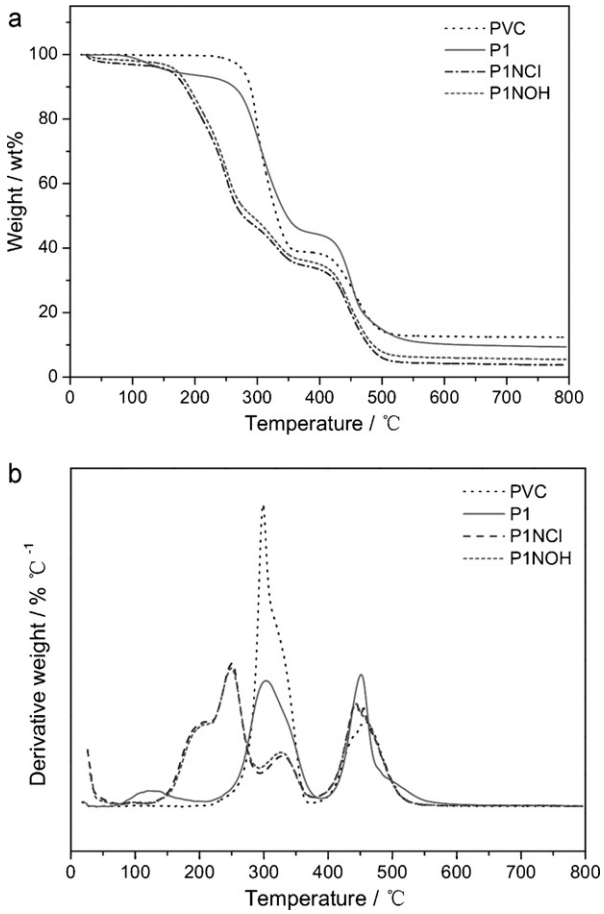

Fig. 5. (a) TGA and (b) DrTGA of PVC, P1, P1NCl and P1NOH membranes.

3.2. Thermal stability and grafting percent of VBC

There are three steps in fabrication of PVC-based plasma grafted alkaline anion-exchange membrane: plasma grafting, quaternization and alkalization. The plasma grafting is the most important step since the contents of quaternary ammonium groups in the membrane could be determined by the grafting percent of VBC. In order to calculate the amount of VBC grafted on PVC, PVC and P1 membranes were characterized by TGA methods, shown in Fig. 5. According to the TGA and its differential (DrTGA) curve, PVC decomposed mainly in two steps, with the first step in the range of 217–380 °C attributed to the dehydrochlorination followed by the formation of conjugated polyene sequence, and the second step in the range of 380–537 °C related to the thermal cracking of the carbonaceous conjugated polyene sequences [38]. There are three major weight loss stages for the P1 membrane: stage (1) in the range of 73–217 °C corresponded to the degradation of trapped VBC monomer [15]; stage (2) in the range of 217–380 °C related to the dehydrochlorination from the C–C backbone and benzyl chloride group; stage (3) in the range of 380–608 °C attributed to the decomposition of polymer's carbon chains and phenyl groups [39]. The degree of grafting can be estimated from the variation of dehydrochlorination between PVC and P1, due to their difference in chloride contents. Eq. (4) shows the relationship among the chloride contents of PVC powder ($\omega_{Cl,PVC}$), VBC monomer ($\omega_{Cl,VBC}$), and P1 membrane ($\omega_{Cl,P1}$).

$$\omega_{Cl,VBC} m_{VBC} + \omega_{Cl,PVC} m_{PVC} = \omega_{Cl,P1}(m_{VBC} + m_{PVC}) \quad (4)$$

where m_{VBC} and m_{PVC} are the mass (g) of VBC and PVC in P1. The chloride contents of PVC powder, VBC monomer and P1 are 58.75 wt% (by observed from Fig. 5), 23.28 wt% (by calculated from the VBC formula) and 47.27 wt% (by observed from Fig. 5), respectively. The weight percent of VBC in P1 ($m_{VBC}/(m_{VBC} + m_{PVC})$) can be calculated to be 32.37 wt%, according to Eq. (4).

Fig. 5 also shows the TGA weight-loss curves for the quaternized and alkalinized membranes. In the TG trace of P1NCl and P1NOH membranes, there was a big mass loss in the range of 120–217 °C, related to the loss of the benzyltrimethylammonium groups [39], indicating the steady operation of P1NOH membrane below 100 °C.

Table 1
Thickness, IEC and water uptake of the P1, P1NCl and P1NOH membranes.

Membrane	Thickness (μm)	IEC (mmol g^{-1})	Water uptake (wt%)
P1	14	–	4.70
P1NCl	15	0.18	23.29
P1NOH	20	1.01	65.63

3.3. IEC and water uptake

IEC is performed to determine the capability of hydroxide ion transport, and of course, to evaluate the applicability in ADAFCs of obtained membranes. IEC values of P1NCl and P1NOH membranes are shown in Table 1. The IEC value of P1NOH membrane is 1.01 mmol g^{-1}, which is higher than that of P1NCl membrane (0.18 mmol g^{-1}), indicating the introduction of functional groups in the alkalinized membrane. The membrane thickness, measured by micrometer (Mitutoyo, Japan), and water uptake values of the hybrid P1, P1NCl and P1NOH membranes agree with this observation, shown in Table 1. The alkalized membrane P1NOH showed the highest water uptake (65.63%), followed by the quaternized membrane P1NCl (23.29%) and plasma-grafted membrane P1 (4.70%). The high water uptake and IEC values of the alkalinized membrane could provide sufficient water molecules to transport OH^- ions through the membrane, indicating excellent ionic conductivity of the P1NOH membrane.

3.4. Ionic conductivity

Hydroxide ion conductivity of the AAEM is a crucial criterion for evaluating its performance in ADAFCs. Fig. 6(a) shows the Nyquist plot of ($-Z''$ versus Z') for the P1NOH membrane measured in deionized water, fitted by the equivalent circuit. The OH^- ion conductivity of the membrane (σ_{OH^-}) can be calculated by Eq. (3) from the AC impedance data. The resistance of P1NOH membrane R_m is 17305 Ω in the hydrated membrane thickness of 20 μm at 20 °C. The OH^- ion conductivity of P1NOH membrane is 0.0145 S cm^{-1}, according to Eq. (3), which is in the range of 0.01–0.02 S cm–1 as reported in the literature, indicating the satisfactory for application of the membrane in fuel cell [15].

Previous studies have demonstrated that the ionic conductivities of ion-exchange membranes are temperature dependence [40–43]. Fig. 6(b) shows the relationship between ln σ_{OH^-} and 1000/T (T is the absolute temperature in Kelvins). Ionic conductivity of P1NOH membrane increases with increasing temperature, assuming that the conductivity followed the Arrhenius law. The anion transport activation energy (E_a) of the P1NOH membrane, which corresponds to the energy barrier for carrier transfer from one free site to another, can be obtained according to the Arrhenius equation:

$$E_a \text{ (kJ mol}^{-1}) = RT^2 \frac{d \ln \sigma_{OH^-}}{dT} \quad (5)$$

where R is the pure gas constant. The activation energy value for alkalinized P1NOH membrane is 13.20 kJ mol^{-1}. The high σ_{OH^-} and low E_a values might be attributed to the high water uptake and

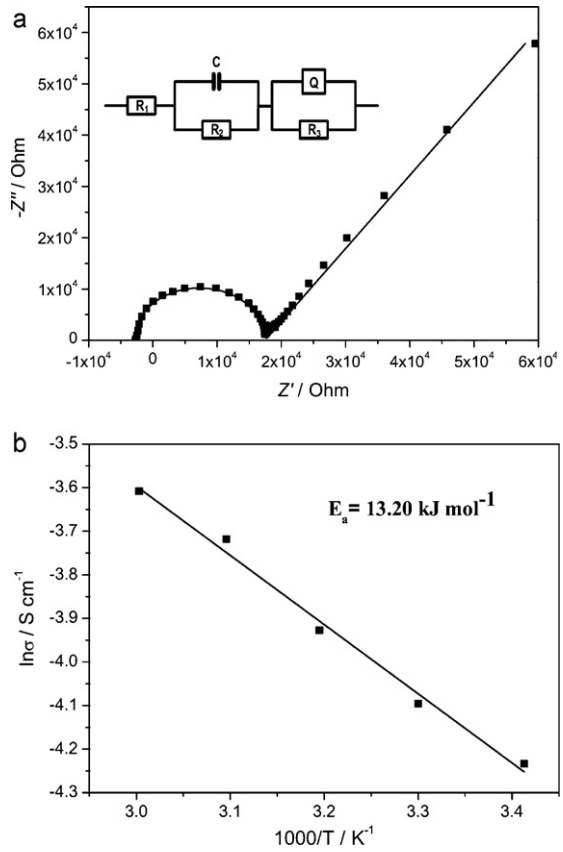

Fig. 6. (a) Nyquist plot for P1NOH membrane and an equivalent circuit. The dots are the experimental results and the curve is the fitting of the experimental results using the equivalent circuit. (b) Temperature dependence of hydroxide ion conductivity for the P1NOH membrane.

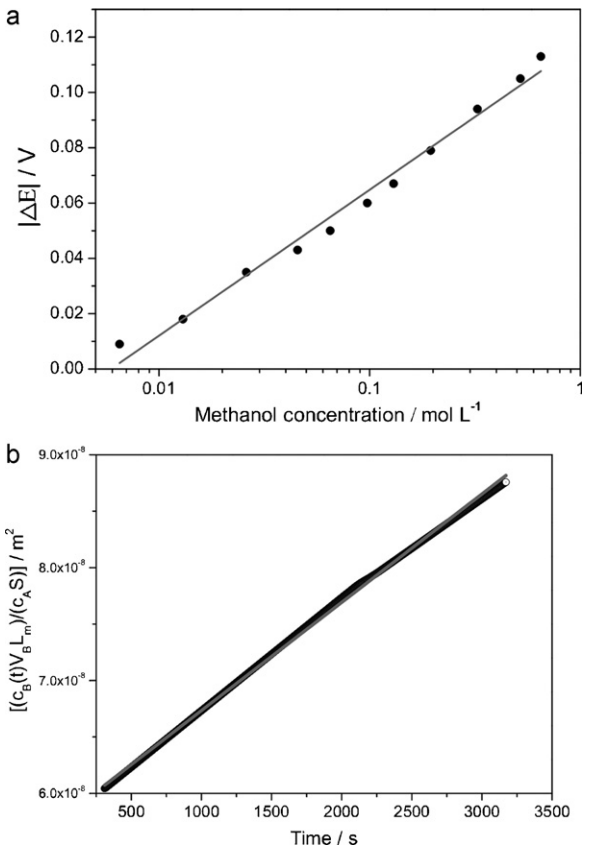

Fig. 7. (a) Potential shift against methanol concentration. The dots are the experimental data and the line is the linear fitting of the experimental results using Eq. (6). (b) Permeability data for the P1NOH membrane in the methanol concentration in compartment A of 1 mol L^{-1} at 20 °C.

IEC of the membrane, which conduce to forming continuous ion transferring channel and make the movement of ion easily [12].

3.5. Methanol permeability

Alcohol permeability of polymer electrolyte membranes is another determinant for potential use in DAFCs due to its influence on the fuel cell power density, energy conversion efficiency and fuel utilization. As mentioned in the experimental section, the measurement of methanol permeability through the P1NOH membrane, in this study, was conducted by an open circuit potential method [22–24]. In the absence of methanol, the potential of GDE in 1 M KOH solution represents the standard electrode potential (E^{θ}). When adding the methanol into the 1 M KOH solution, the potential of GDE drops, according to the concentration of methanol, due to the oxidation of methanol in the Pt catalyst surface. There is a relationship between the variation of GDE potential (ΔE) and the concentration of methanol (c_{CH_3OH}), shown in Eq. (6).

$$\Delta E = -a \ln c_{CH_3OH} \quad (6)$$

where a is a constant. The calibration curve of potential shift against methanol concentration is shown in Fig. 7(a). Therefore, the methanol concentration in compartment B during permeation experiment can be inferred from the variation of GDE using Eq. (6).

Eq. (7) shows the relationship between the concentration of methanol in compartment B ($c_{CH_3OH,B}$ in mol L^{-1}) and permeation time (t in s) [21].

$$\frac{V_B L_m}{c_{CH_3OH,A} S} c_{CH_3OH,B}(t) = P\left(t + \frac{L_m^2}{6D}\right) \quad (7)$$

where P, D, L_m and S are the methanol permeability ($m^2\ s^{-1}$), diffusion coefficient ($m^2\ s^{-1}$), membrane thickness (m) and membrane active area (m^2) of P1NOH membrane, respectively. V_B and $c_{CH_3OH,A}$ are the volume of compartment B (m^3) and concentration of methanol in compartment A (mol L^{-1}), respectively. It is evident that $(V_B L_m / c_{CH_3OH,A} S) c_{CH_3OH,B}(t)$ has a linear correlation with the permeation time, shown in Fig. 7(b). The slope and intercept of the fitting line are methanol permeability (P) and $P(L_m^2/6D)$, respectively. The methanol permeability of P1NOH membrane, based on Fig. 7(b), is 9.59×10^{-12} $m^2\ s^{-1}$ when the concentration of methanol in compartment A is 1 mol L^{-1}. There are mainly two factors affecting methanol permeation: the diffusion and electro-osmotic drag. However, in alkaline direct methanol fuel cells ion transport through the membrane occurs in the direction opposite to the methanol crossover, which leads to the decrease of electro-osmotic drag. The diffusion coefficient (D) of P1NOH membrane is only 1.11×10^{-14} $m^2\ s^{-1}$, based on Fig. 7(b) and Eq. (7). The low methanol permeability and diffusion coefficient value suggested a good performance of P1NOH membrane for application in ADAFCs.

3.6. Chemical stability

Membrane chemical stability is generally characterized by durability time [39]. Since the alkaline anion-exchange membranes work in oxidative circumstances, the chemical stability of AAEM has often been evaluated in strong oxidative conditions, such as 3 wt% H_2O_2 [44]. The change in the weight content of the P1NOH membrane in 3 wt% H_2O_2 over time is shown in Fig. 8. In the first 50 h, the weight loss of P1NOH membrane was 6.67 wt% due to the trapped free radicals within the polymer backbone by plasma

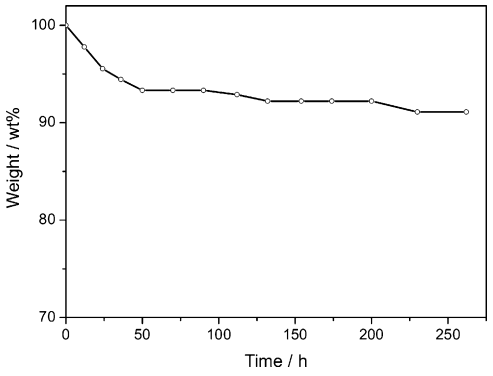

Fig. 8. The oxidative stability of the P1NOH membrane.

bombardment [45]. In the next 121 h, the weight loss of P1NOH membrane was only 2.22 wt%, suggesting that the structure of the polymer matrix was not destroyed by the plasma treatment. The chemical stability of P1NOH membrane was acceptable [46].

3.7. Mechanical properties

The mechanical properties of dried P1, P1NOH membranes (RH 0%) and fully hydrated P, P1NOH membranes (RH 100%) were evaluated using tensile stress-strain measurements. The TS, E_b and tensile modulus values are collected in Table 2. The P1NOH membranes withstand lower tensile stresses than the P1 precursor membrane, indicating the influence of the quaternization and alkalization progresses on the membrane mechanical properties. The fully hydrated P1NOH membrane exhibited TS with an average 8.74 MPa of stress resulting in 5.1% strain. Compared to the values in literatures, the mechanical properties of our membranes can be acceptable [18,47].

3.8. ADAFC performance

The cell voltage and power density curves of ADAFCs with 1–2 M EtOH solution using P1NOH membrane as the electrolyte are presented in Fig. 9. The fuel cell containing P1NOH membrane exhibited open circuit voltages (OCVs) of 0.796 V and 0.788 V in 1 M and 2 M EtOH solution, respectively. The open circuit voltages of the cells using P1NOH membrane were stabilized within the range of 0.75–0.80 V, which were about 100 mV higher than that of the ADMFC with radiation-grafted AAEM in the absence of KOH in anode fuel solution [18]. This may be due to the undamaged polymer backbone structure and good alcohol resistance of the P1NOH membrane. The OCV slightly decreased with increasing EtOH concentration from 1 M to 2 M due to the higher EtOH crossover [48]. It is difficult to compare directly the cell performance in our test to literature values, as the ADAFC studies have used EtOH solution containing KOH. From Fig. 9, it is immediately evident that the power densities produced in our study were a little poorer than that of the Ref. in the absence of KOH in anode fuel solution [18]. There are a number of reasons to affect the fuel cell performance, such as the kind of catalyst, catalyst loading, testing condition (alcohol fuel containing KOH or not, KOH concentration, alcohol concentration

Table 2
The mechanical properties of the P1 and P1NOH membranes.

Membrane	TS (MPa)	E_b (%)	Tensile modulus (MPa)
P1, RH 0%	12.71	2.5	996.3
P1, RH 100%	27.33	6.1	1601.0
P1NOH, RH 0%	9.16	1.4	618.6
P1NOH, RH 100%	8.74	5.1	374.7

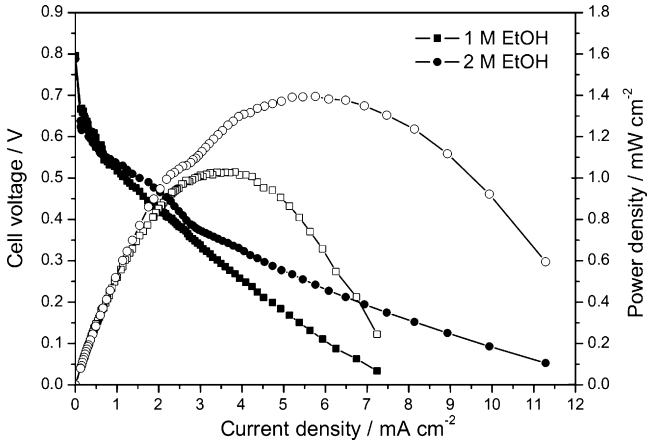

Fig. 9. Cell voltage and power density vs. current density for the air-breathing fuel cell with P1NOH membrane using 1 M ethanol (■) and 2 M ethanol (●) at room temperature. (Anode: 0.40 mg Pt cm^{-2}; cathode: 0.20 mg Pt cm^{-2}.)

and flow rate, O_2 concentration and flow rate) and so on. Further researches on the comprehensive evaluation of the ADAFC performance using the plasma-grafted AAEMs are under investigation.

4. Conclusions

In this study, we adopted a novel technique to prepare AAEMs based on PVC powders via plasma grafting, quaternization and alkalization. The TGA, ATR-FTIR and XPS analysis demonstrate that the benzyltrimethylammonium cationic groups have been successfully introduced into the PVC polymer matrix. TGA analysis also indicates that the plasma-grafted AAEMs can be used safely at <100 °C. The structure of the polymer matrix was not destroyed by the plasma treatment. Due to the high water uptake and satisfactory IEC, the P1NOH membrane exhibits an excellent hydroxide ion conductivity (0.0145 S cm^{-1} in deionized water at 20 °C). The methanol permeability (9.59×10^{-12} m^2 s^{-1}) suggests that the P1NOH membrane has good methanol resistance. The open circuit voltage of air-breathing ADAFC using this newly AAEM is 0.796 V with 1 M EtOH solution at ambient temperature. This performance criterion expects that such kind of plasma-grafted AAEMs have great potential for application in alkaline directly alcohol fuel cells.

Acknowledgements

This research is financially supported by the Institute of Plasma Physics, Chinese Academy of Sciences (No. Y05FCQ1128; No. 095GZ1156Y), the National Nature Science Foundation of China (No. 10975162) and Core-University program of Japan-China.

References

[1] Y. Wang, L. Li, L. Hu, L. Zhuang, J. Lu, B. Xu, Electrochem. Commun. 5 (2003) 662–666.
[2] M. Sevilla, C. Sanchís, T. Valdés-Solís, E. Morallón, A.B. Fuertes, Electrochim. Acta 54 (2009) 2234–2238.
[3] E.H. Yu, K. Scott, J. Power Sources 137 (2004) 248–256.
[4] E. Antolini, J. Power Sources 170 (2007) 1–12.
[5] S.F. Lu, J. Pan, A.B. Huang, L. Zhuang, J.T. Lu, Proc. Natl. Acad. Sci. U.S.A. 105 (2008) 20611–20614.
[6] J.R. Varcoe, R.C.T. Slade, G.L. Wright, Y.L. Chen, J. Phys. Chem. B 110 (2006) 21041–21049.
[7] C. Coutanceau, L. Demarconnay, C. Lamy, J.M. Leger, J. Power Sources 156 (2006) 14–19.
[8] J.R. Varcoe, R.C.T. Slade, Fuel Cells 5 (2005) 187–200.
[9] K. Kordesch, J.C.T. Oliveira, Int. J. Hydrogen Energy 13 (1988) 411–427.
[10] G.-J. Hwang, H. Ohya, J. Membr. Sci. 149 (1998) 163–169.
[11] E.N. Komkova, D.F. Stamatialis, H. Strathmann, M. Wessling, J. Membr. Sci. 244 (2004) 25–34.
[12] Y. Xiong, J. Fang, Q.H. Zeng, Q.L. Liu, J. Membr. Sci. 311 (2008) 319–325.

[13] G.G. Wang, Y.M. Weng, D. Chu, D. Xie, R.R. Chen, J. Membr. Sci. 326 (2009) 4–8.
[14] T. Xu, Z. Liu, W. Yang, J. Membr. Sci. 249 (2005) 183–191.
[15] T.N. Danks, R.C.T. Slade, J.R. Varcoe, J. Mater. Chem. 13 (2003) 712–721.
[16] H. Herman, R.C.T. Slade, J.R. Varcoe, J. Membr. Sci. 218 (2003) 147–163.
[17] J.R. Varcoe, Phys. Chem. Chem. Phys. 9 (2007) 1479–1486.
[18] J.R. Varcoe, R.C.T. Slade, E.L.H. Yee, S.D. Poynton, D.J. Driscoll, D.C. Apperley, Chem. Mater. 19 (2007) 2686–2693.
[19] H. Yasuda, Plasma Polymerization, first ed., Acadamic Press, Inc., Orlando, Florida, 1985.
[20] R.K. Nagarale, G.S. Gohil, V.K. Shahi, R. Rangarajan, Macromolecules 37 (2004) 10023–10030.
[21] Z. Jiang, Z.-j. Jiang, X. Yu, Y. Meng, Plasma Process. Polym. 7 (2010) 382–389.
[22] Z. Wu, G. Sun, W. Jin, Q. Wang, H. Hou, K.-Y. Chan, Q. Xin, J. Power Sources 167 (2007) 309–314.
[23] N. Munichandraiah, K. McGrath, G.K.S. Prakash, R. Aniszfeld, G.A. Olah, J. Power Sources 117 (2003) 98–101.
[24] J. Liu, H. Wang, S. Cheng, K.-Y. Chan, J. Membr. Sci. 246 (2005) 95–101.
[25] S. Rajendran, T. Uma, J. Power Sources 88 (2000) 282–285.
[26] D.O.H. Teare, D.C. Barwick, W.C.E. Schofield, R.P. Garrod, L.J. Ward, J.P.S. Badyal, Langmuir 21 (2005) 11425–11430.
[27] N. Sundaraganesan, H. Saleem, S. Mohan, M. Ramalingam, V. Sethuraman, Spectrochim. Acta A 62 (2005) 740–751.
[28] E. Loubaki, M. Ourevitch, S. Sicsic, Eur. Polym. J. 27 (1991) 311–317.
[29] Y. Yamaguchi, T.T. Nge, A. Takemura, N. Hori, H. Ono, Biomacromolecules 6 (2005) 1941–1947.
[30] L. Sun, Y. Du, L. Fan, X. Chen, J. Yang, Polymer 47 (2006) 1796–1804.
[31] E. Papirer, R. Lacroix, J.-B. Donnet, G. Nanse, P. Fioux, Carbon 33 (1995) 63–72.
[32] D. Briggs, G. Beamson, Anal. Chem. 64 (1992) 1729–1736.
[33] T.I.T. Okpalugo, P. Papakonstantinou, H. Murphy, J. McLaughlin, N.M.D. Brown, Carbon 43 (2005) 153–161.
[34] F.J. Xu, E.T. Kang, K.G. Neoh, Macromolecules 38 (2005) 1573–1580.
[35] K.L. Tan, B.T.G. Tan, E.T. Kang, K.G. Neoh, J. Mater. Sci. 27 (1992) 4056–4060.
[36] A. Welle, J.D. Liao, K. Kaiser, M. Grunze, U. Mäder, N. Blank, Appl. Surf. Sci. 119 (1997) 185–198.
[37] Z. Shi, K.G. Neoh, E.T. Kang, Biomaterials 26 (2005) 501–508.
[38] J. Liu, G. Chen, J. Yang, L. Ding, Mater. Chem. Phys. 118 (2009) 405–409.
[39] Y. Wu, C. Wu, T. Xu, F. Yu, Y. Fu, J. Membr. Sci. 321 (2008) 299–308.
[40] C.C. Yang, J. Membr. Sci. 288 (2007) 51–60.
[41] L. Li, Y. Wang, J. Membr. Sci. 262 (2005) 1–4.
[42] B.P. Tripathi, M. Kumar, V.K. Shahi, J. Membr. Sci. 360 (2010) 90–101.
[43] Y. Xiong, Q.L. Liu, A.M. Zhu, S.M. Huang, Q.H. Zeng, J. Power Sources 186 (2009) 328–333.
[44] Y. Xiong, Q.L. Liu, Q.H. Zeng, J. Power Sources 193 (2009) 541–546.
[45] H. Biederman, Plasma Polymer Films, Imperial College Press, Covent Gardent, London, 2004.
[46] Z. Jiang, X. Zheng, H. Wu, F. Pan, J. Power Sources 185 (2008) 85–94.
[47] T.J. Clark, N.J. Robertson, H.A. Kostalik Iv, E.B. Lobkovsky, P.F. Mutolo, H.c.D. Abruña, G.W. Coates, J. Am. Chem. Soc. 131 (2009) 12888–12889.
[48] J.H. Kim, H.K. Kim, K.T. Hwang, J.Y. Lee, Int. J. Hydrogen Energy 35 (2010) 768–773.